

FAM181A and FAM181B, two new TEAD interactors.

Fedir Bokhovchuk^{1#}, Yannick Mesrouze^{1#}, Clara Delaunay¹, Typhaine Martin¹, Frédéric Villard², Marco Meyerhofer¹, Patrizia Fontana¹, Catherine Zimmermann¹, Dirk Erdmann¹, Pascal Furet³, Clemens Scheufler², Tobias Schmelzle¹ and Patrick Chène^{1*}.

¹Disease Area Oncology, ²Chemical Biology & Therapeutics and ³Global Discovery Chemistry, Novartis Institutes for Biomedical Research, Basel, Switzerland.

Supplementary Table

	FAM181A ¹⁹⁰⁻²⁰⁵ :TEAD4 ²¹⁷⁻⁴³⁴ PDB 6SEN	FAM181B ²²⁰⁻²³⁵ :TEAD4 ²¹⁷⁻⁴³⁴ PDB 6SEO
Data collection^a		
Space group	C ₂	H3 ₂
Cell (Å, deg)	a=66.5, b=132.1, c=62.0, β=115.9	a=b=135.9, c=88.7
Resolution (Å)	1.61 (1.73-1.61) ^b	2.52 (2.64-2.52) ^b
R _{merge} , all (%)	3.8 (83.5)	11.2 (224.9)
Mean I/σ(I)	14.3 (1.4)	15.5 (1.1)
Completeness spherical (%)	77.0 (20.1)	72.5 (28.0)
Completeness ellipsoidal (%)	93.7 (63.4)	95.0 (81.7)
Multiplicity	3.4 (3.5)	10.1 (10.2)
Refinement^c		
Resolution (Å)	25 - 1.65	30 - 2.55
No. reflections	47141	7693
R _{work} / R _{free} (%)	19.0 / 21.9	18.3 / 23.2
R.m.s deviations bond lengths (Å)	0.010	0.010
R.m.s deviations bond angles (deg)	1.09	1.2
Complex molecules in AU	2	1
Myristate	Covalent ^d	Covalent ^d

Supplementary Table 1. Crystallographic data collection and refinement statistics for the FAM181A/B:TEAD4 complexes. ^a. Values as reported in autoPROC ¹. ^b. Highest resolution shell is shown in parentheses. ^c. Values as defined in BUSTER (Global Phasing Ltd., UK). ^d. The myristate was modeled covalently bound to Lys344^{TEAD4}.

Supplementary Figures

Supplementary Fig. S1. Sequences of the motifs used to interrogate the databases. See Material and Methods for explanations. The residues in red indicate the positions for which the identification of alternative amino acids is evaluated in the corresponding motif search.

Supplementary Fig. S2. Inhibition curves obtained in the TR-FRET assay. The ability of the different peptides or protein fragments to inhibit the YAP:TEAD interaction was measured in a TR-FRET assay. Twelve stepwise dilutions (dilution factor 3.33) of each peptide/protein fragment were used in the experiments. The highest concentrations present in the assay were 222 μM for FAM181A¹⁹⁰⁻²⁰⁵, FAM181B²²⁰⁻²³⁵ or YAP⁸⁴⁻⁹⁹; 250 μM for YAP⁸⁵⁻⁹⁹; 55 μM for FAM181A¹²⁷⁻²⁰⁵; 125 μM for FAM181B¹⁵⁷⁻²³⁷. The IC₅₀ values were estimated by nonlinear regression analysis with GraphPad Prism (GraphPad Software, San Diego, CA). The stars indicate the signal measured in the absence of the peptide or protein fragments.

Supplementary Fig. S3. LC-MS analyses of FAM181A¹²⁷⁻²⁰⁵ and FAM181B¹⁵⁷⁻²³⁷. The figure represents HPLC profiles obtained with the purified FAM181A¹²⁷⁻²⁰⁵ and FAM181B¹⁵⁷⁻²³⁷ fragments. The numbers indicate the mass measured by mass spectrometry. The theoretical molecular weight calculated from the primary sequence are given in brackets. The amount of sample used for the analysis is indicated.

Supplementary Fig. S4. Binding of FAM181B¹⁵⁷⁻²³⁷ and FAM181A¹²⁷⁻²⁰⁵ to wt^{TEAD4}, Val389Ala^{TEAD4} and Asp272Ala^{TEAD4}. The biotinylated N-Avitagged TEAD4 proteins were immobilized on sensor chips, and the binding of different concentrations of FAM181B¹⁵⁷⁻²³⁷ or FAM181A¹²⁷⁻²⁰⁵ was measured at 298°K by Surface Plasmon Resonance. The upper panels show representative sensorgrams and the lower panels the corresponding binding isotherms from which K_d values (at equilibrium) were derived (excepted for Asp272Ala^{TEAD4}). The sensorgrams were globally fitted with a 1:1 interaction model using the Biacore T200

evaluation software (Biacore, Sweden). The concentrations used are indicated. The signal measured at equilibrium (R_{\max}^{eq}) and the calculated maximum feasible signal (R_{\max}^{th}) are given. Only apparent K_d values were determined with FAM181A¹²⁷⁻²⁰⁵ (see text).

Supplementary Fig. S5. Molecular dynamics simulation of the FAM181B¹⁵⁴⁻²³⁶:TEAD4²¹⁷⁻⁴³⁴ complex. The simulation of molecular dynamics was run using the Desmond module (Maestro package, Schrodinger Inc., Cambridge, MA). Ten snapshots of the 10 ns molecular dynamics simulation are shown. The initial, intermediate and final conformations of FAM181B¹⁵⁴⁻²³⁶ are in blue, orange and green, respectively. TEAD4²¹⁷⁻⁴³⁴ is represented in gray. The different secondary structure elements of FAM181B¹⁵⁴⁻²³⁶ are indicated. The picture was drawn with PyMOL (Schrödinger Inc., Cambridge, MA).

Supplementary Fig. S6. Structural study of FAM181A/B. **A.** Circular dichroism (CD) analysis of FAM181A¹²⁷⁻²⁰⁵ and FAM181B¹⁵⁷⁻²³⁷. The proteins were dialyzed in 20 mM phosphate buffer pH 7.4, 100 mM KF, 0.25 mM TCEP and diluted in this buffer to 0.2 mg.mL⁻¹. Far-UV CD spectra were recorded as previously described². TEAD4²¹⁷⁻⁴³⁴ was used as an example of folded protein. The figure represents the average CD spectrum obtained from two independent experiments. **B.** PrDos analysis of full length FAM181A/B. The primary sequences of FAM181A (UniProt Q8N9Y4) and FAM181B (UniProt A6NEQ2) were analyzed with the protein disorder prediction server PrDOS (<http://prdos.hgc.jp>)³ using the default settings. The upper panels are graphic representations of the disorder probability calculated for each residue. A probability score higher than 0.5 suggests that the residue is located in a disordered area. The lower panels correspond to the primary sequence of the two proteins with the residues located in regions predicted to be disordered indicated in red. The green arrows indicate FAM181A¹²⁷⁻²⁰⁵ and FAM181B¹⁵⁷⁻²³⁷.

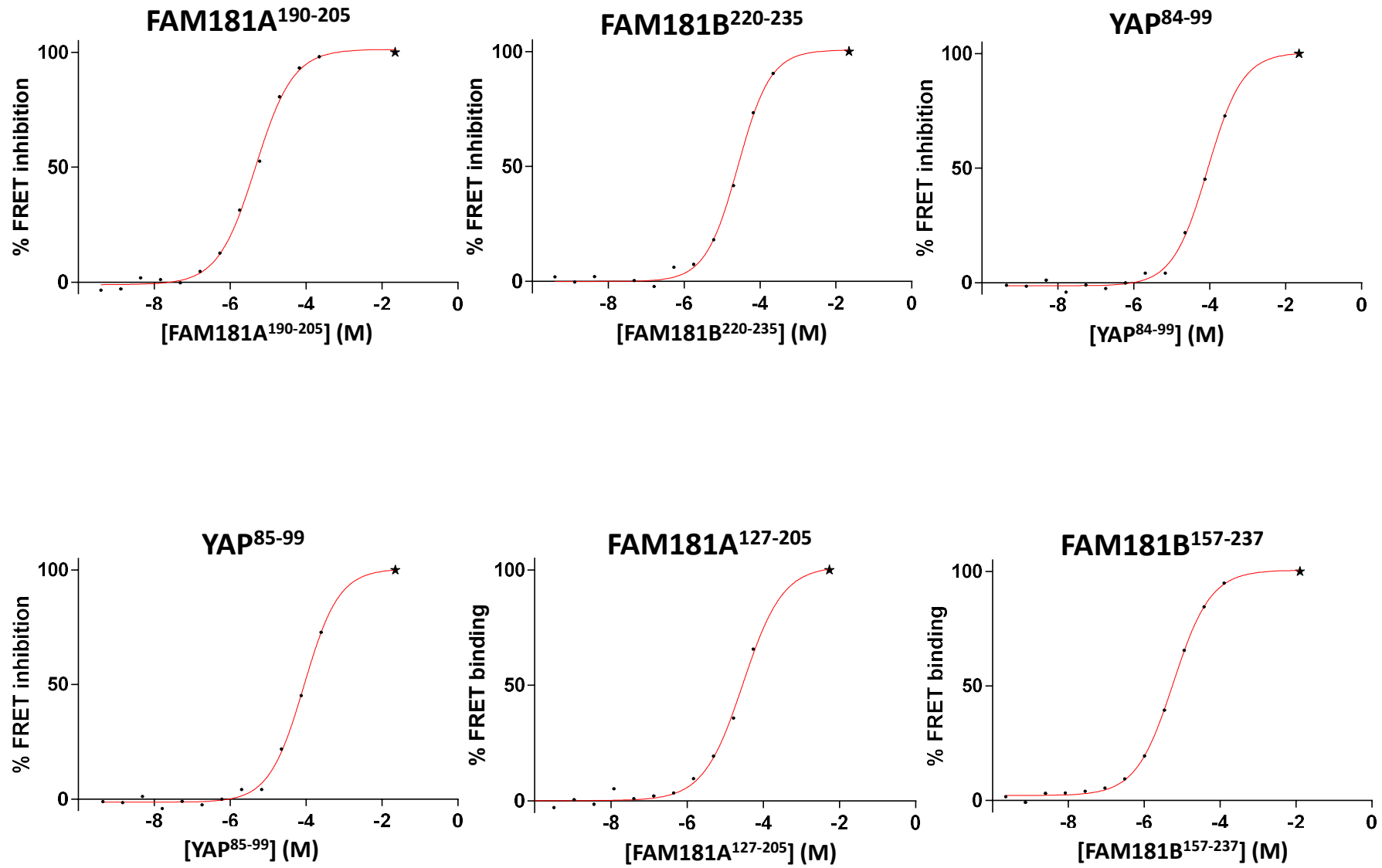
References

1. Vonrhein C, Flensburg C, Keller P, Sharff A, Smart O, Paciorek W, Womack T, Bricogne G (2011) Data processing and analysis with the autoPROC toolbox. *Acta Crystallogr Sect D* 67:293-302.
2. Mesrouze Y, Bokhovchuk F, Meyerhofer M, Fontana P, Zimmermann C, Martin T, Delaunay C, Erdmann D, Schmelzle T, Chène P (2017) Dissection of the interaction between the intrinsically disordered YAP protein and the transcription factor TEAD. *eLife* 6:e25068.
3. Ishida T, Kinoshita K (2007) PrDOS: prediction of disordered protein regions from amino acid sequence. *Nucl Acids Res* 35:W460-W464.

Supplementary Fig. S1

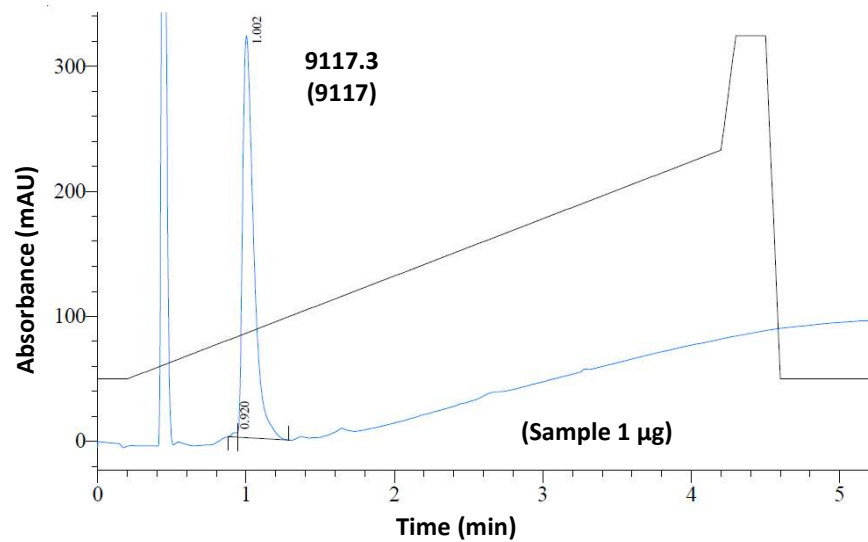
	Corresponding positions in YAP ⁸⁵⁻⁹⁹														
	85	86	87	88	89	90	91	92	93	94	95	96	97	98	99
Motif_01	P	x	R	x	R	x	[LM]	P	x	{S}	F	F	x	x	P
Motif_02	P	x	R	x	R	x	[LM]	P	x	S	{F}	F	x	x	P
Motif_03	P	x	R	x	R	x	[LM]	P	x	S	F	{F}	x	x	P
Motif_04	P	x	R	x	R	x	{LM}	P	x	S	F	F	x	x	P
Motif_05	{P}	x	R	x	R	x	[LMF]	P	x	S	F	[FW]	x	x	P
Motif_06	P	x	{R}	x	R	x	[LMF]	P	x	S	F	[FW]	x	x	P
Motif_07	P	x	[RKHS]	x	{R}	x	[LMF]	P	x	S	F	[FW]	x	x	P
Motif_08	P	x	[RKHS]	x	R	x	[LMF]	P	x	{S}	F	[FW]	x	x	P
Motif_09	P	x	[RKHS]	x	R	x	[LMF]	P	x	S	{F}	[FW]	x	x	P
Motif_10	P	x	[RKHS]	x	R	x	[LMF]	{P}	x	S	F	[FW]	x	x	P
Motif_11	{P}	x	[RKHS]	x	R	x	[LMF]	P	x	S	F	[FW]	x	x	P
Motif_12	P	x	[RKHS]	x	R	x	[LMF]	P	x	S	F	[FW]	x	x	{P}
Motif_13	P	x	[RKHS]	x	R	x	[LMF]	P	x	S	F	{FW}	x	x	P
Motif_14	P	x	[RKHS]	x	R	x	{LMF}	P	x	S	F	[FW]	x	x	P
Final	P	x	[RKHS]	x	R	x	[LMF]	P	x	S	F	[FW]	x	x	P

Supplementary Fig. S2

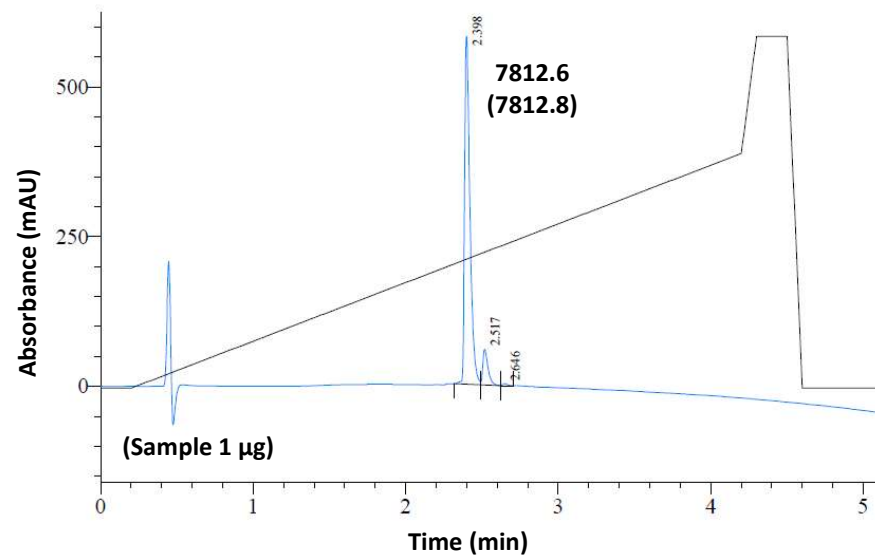


Supplementary Fig. S3

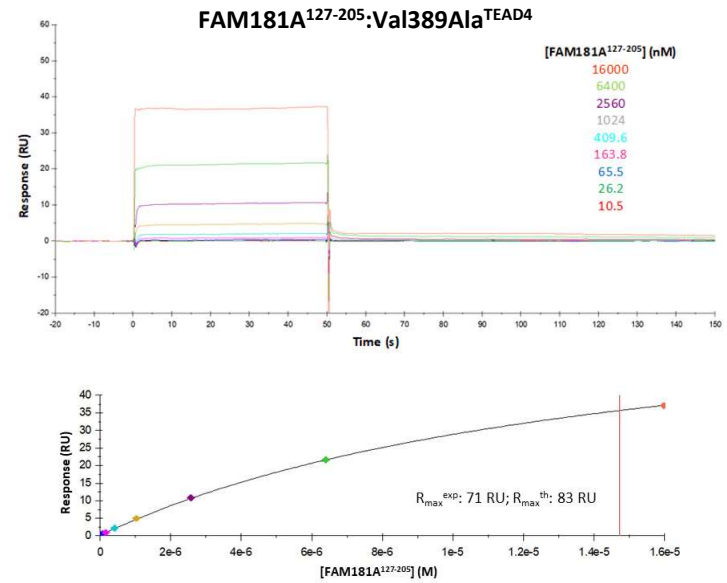
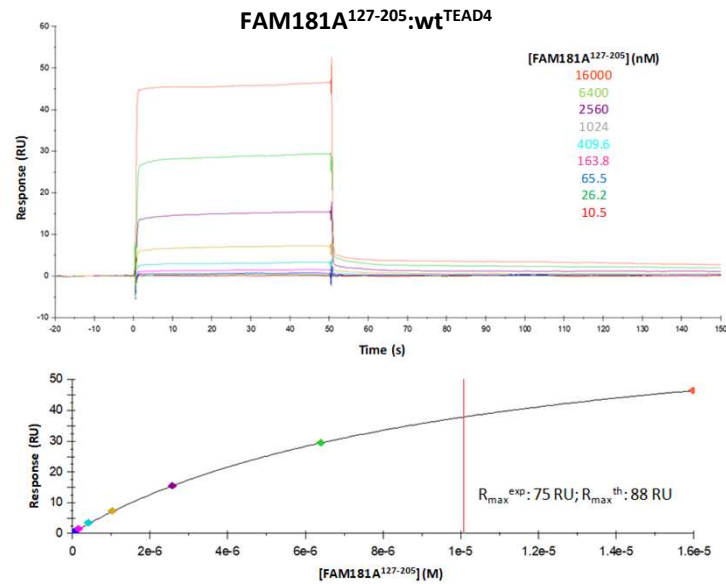
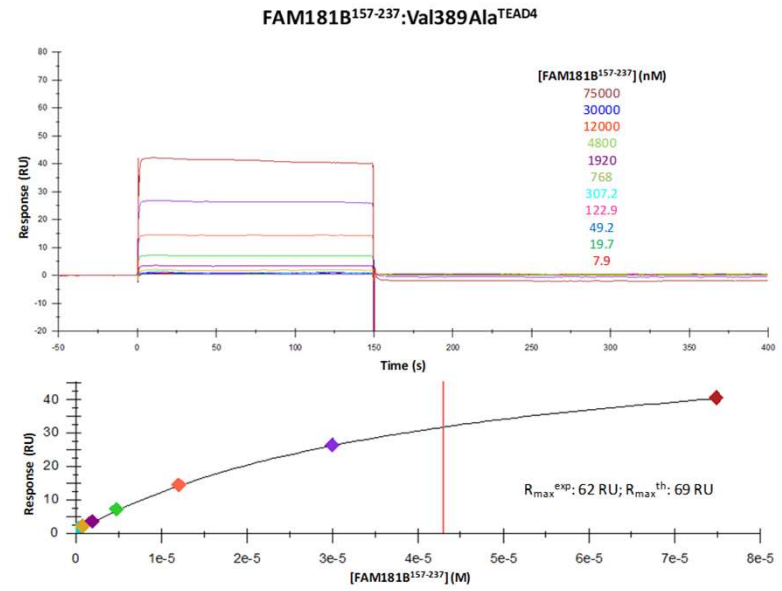
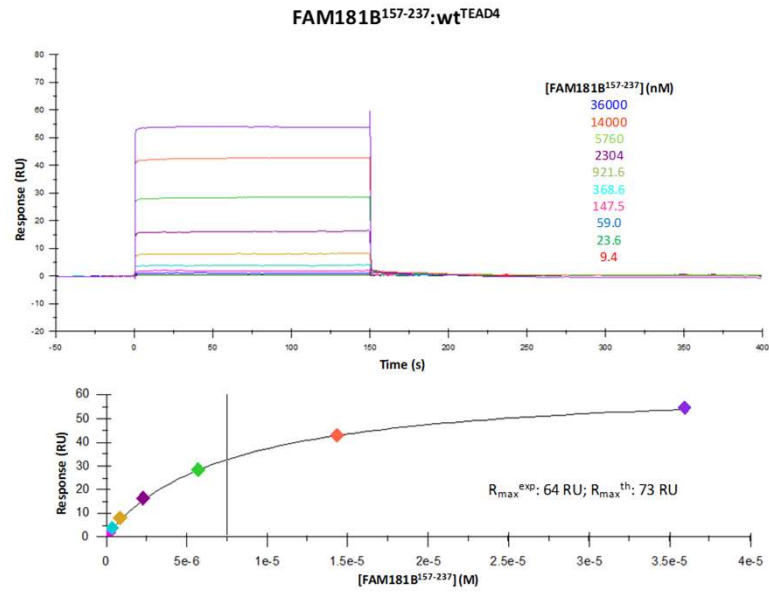
FAM181A¹²⁷⁻²⁰⁵



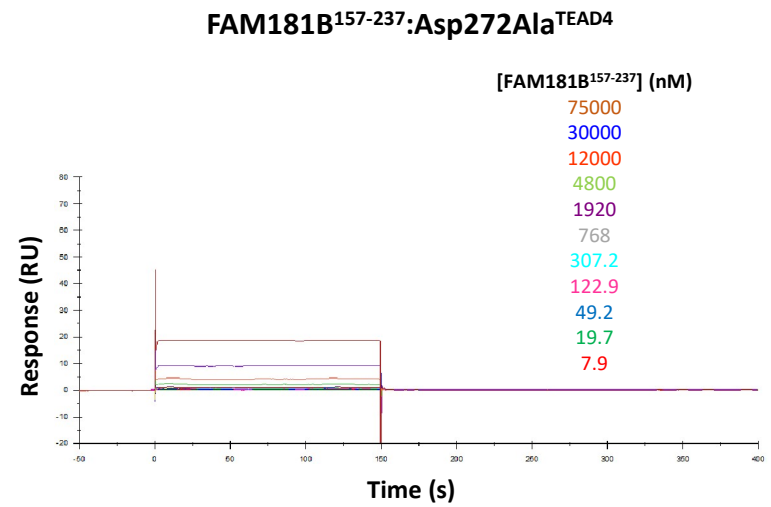
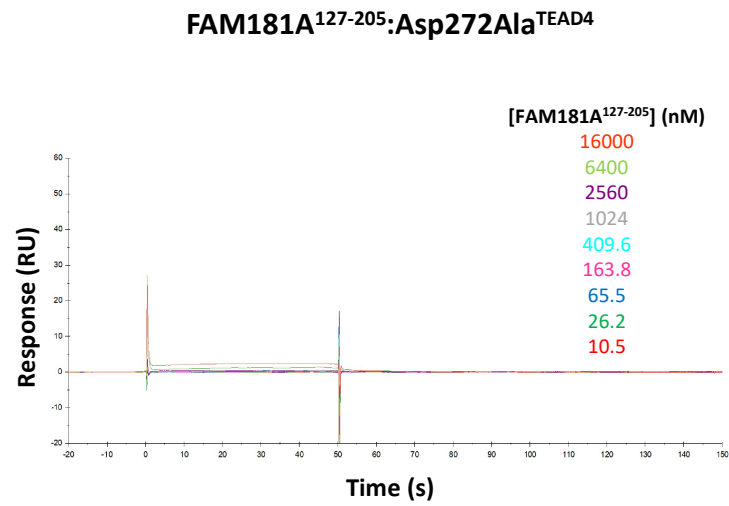
FAM181B¹⁵⁷⁻²³⁷



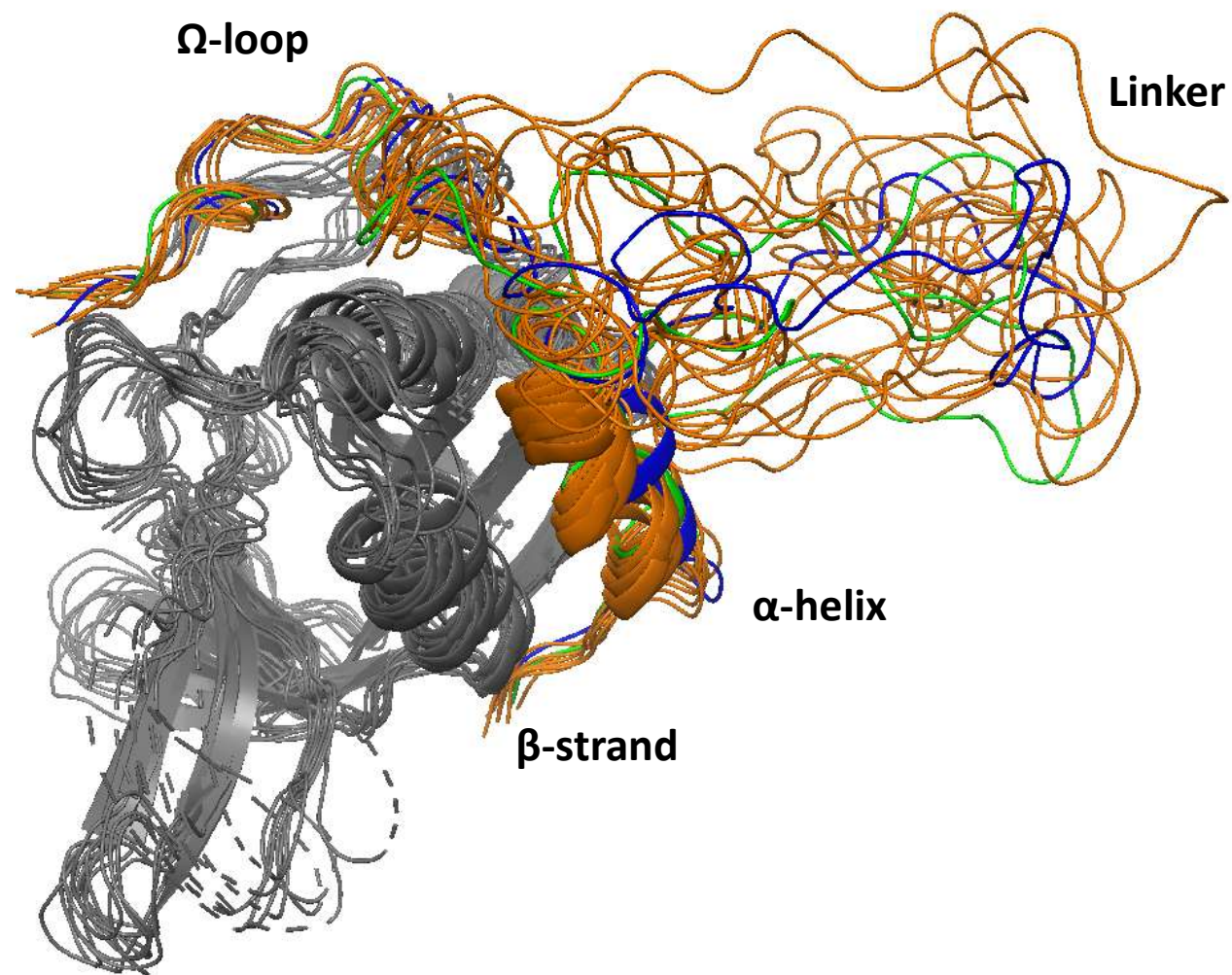
Supplementary Fig. S4



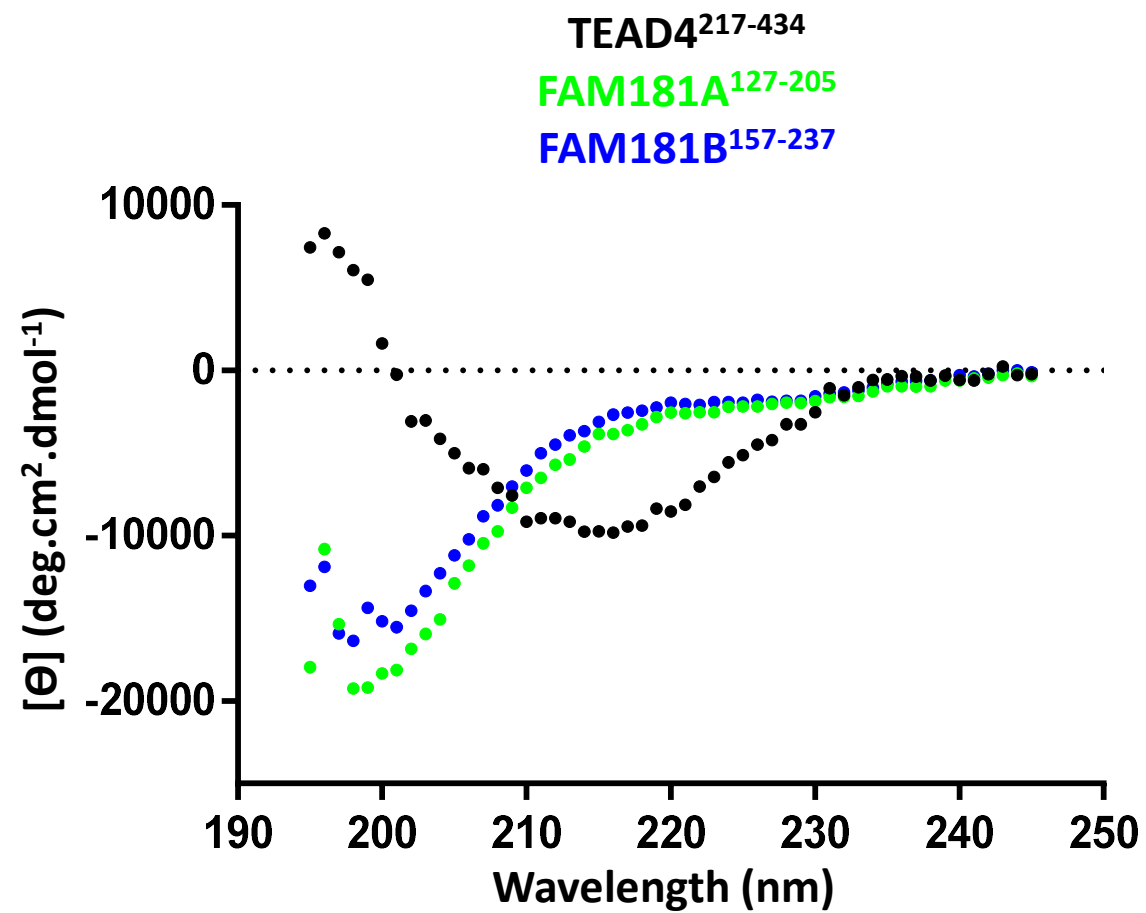
Supplementary Fig. S4



Supplementary Fig. S5

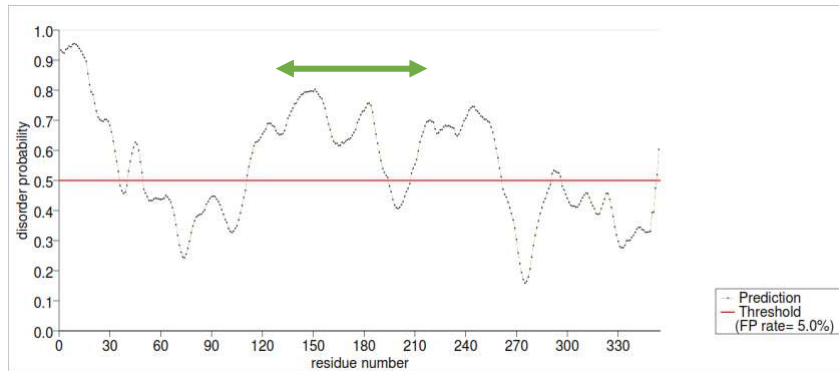


Supplementary Fig. S6A



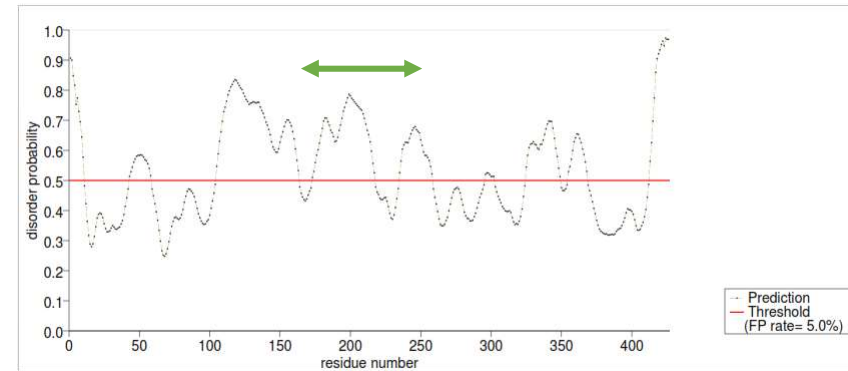
Supplementary Fig. S6B

FAM181A



1	M PLEERRSSG	E RNDAAPT N H	R RPGEKR A ST	A KQVSSV P FL	G AAG H QQ S LP	50
51	SSWKASCSGP	LVMA S DS D VK	MLLN F V N LAS	SDIKAAL D KS	APCRR S VD H R	100
101	KYLQ K QL K R F	S Q K YS R LP R G	L PG R AA E P Y L	K RG S ED R FR R	L LL D L G PD S S	150
151	P GGGG G CK E K	V LR N PY R EE C	L AK E QL P Q R Q	H PEAA Q PG Q V	F MRKR Q LP A S	200
201	F WEE P RP T HS	Y H V GLE G GL G	P REG P Y E G K	K NC K GLE P L G	P ET T LV S M S P	250
251	R AL A E K E P L K	M PGV S LV G RV	N AW S CC P F Q Y	H G Q PI Y PG L	G AL F Q S P V PS	300
301	L GL W R K SP A F	P GEL A HL C K D	V DGL G Q K V C R	P VVL K PI P TK	P AV P PI F N V	350
351	F GY L					400

FAM181B



1	M AV Q A A LL S T	H F F V P F G F G G	S P D G L G G A F G	A L D K G C C F E D	D E T G A P A G A L	50
51	L S G A E G D V R	E A T R D L L S P I	D S A S S N I K L A	L D K P G K S K R K	V N H R K Y L Q K Q	100
101	I K R C S G L M G A	A P F G P P S P S A	A D T P A K R P L A	A P S A P T V A A P	A H G K A P R R E	150
151	A S Q A A A A A S L	Q S R S L A A L F D	S L R H V P G G A E	P A G G E V A A P A	A G L G G A G T G G	200
201	A G G D V A G P A G	A T A I P G A R K V	P L R A R N L P P S	F F T E P S R A G G	G C G P S G F D V	250
251	S L G D L E K G A E	A V E F F E L L G P	D Y G A G T E A A V	L L A E P L D V F	P A G A S V L R G P	300
301	P E L E P G L F E P	P P A V V G N L L Y	P E P W S V P G C S	P T K S P L T A P	R G G L T L N E F L	350
351	S P L Y P A A A D S	P G G E D G R G H L	A S F A P F F P D C	A L P P P P P H Q	V S Y D S A G Y S	400
401	R T A Y S S L W R S	D G V W E G A P G E	E G A H R D			450